



# Phase Diagram of the Pb-Se-Sn System

SINN-WEN CHEN <sup>1,2,4</sup> TSE-YANG HUANG,<sup>1</sup> YA-HSIANG HSU,<sup>1</sup>  
and ALEŠ KROUPA<sup>3</sup>

1.—Department of Chemical Engineering, National Tsing Hua University, Hsin-chu, Taiwan.  
2.—High Entropy Materials Center, National Tsing Hua University, Hsin-chu, Taiwan.  
3.—Institute of Physics of Materials, Czech Academy of Sciences, Brno, Czech Republic.  
4.—e-mail: swchen@mx.nthu.edu.tw

The Pb-Se-Sn ternary system is of interest to thermoelectric applications. Nevertheless, no phase diagram exists for the entire compositional regime at any temperature. Ternary Pb-Se-Sn alloys are equilibrated at 350°C and 500°C, and their equilibrium phases are determined. The isothermal sections of the equilibrium Pb-Se-Sn phase diagram at 350°C and 500°C are proposed based on the phase diagrams of the three constituent binary systems and ternary phase equilibria results in the literature and those determined in this study. No ternary compound is found. The phase relationships are similar at 350°C and 500°C. At both temperatures, binary compounds,  $\alpha$ -PbSe and  $\gamma$ -SeSn, have very significant ternary solubility, but the ternary solubility of Pb in the Se<sub>2</sub>Sn phase is negligible. There are still unresolved questions about the type and shape of the liquid phase at the Se corner.

**Key words:** Phase diagram, Pb-Se-Sn, isothermal section, thermoelectric

## INTRODUCTION

Thermoelectric modules can enhance energy use efficiency by recovering and converting waste heat into electricity. They are also a renewable energy source when used together with solar heating modules. Because of their potential applications, thermoelectric materials and thermoelectric modules have attracted very intensive research interest and efforts.<sup>1–10</sup> The Pb-Se-Sn ternary system is an important material system for thermoelectric applications.  $\alpha$ -PbSe,  $\gamma$ -SeSn and PbSeSn are promising thermoelectric materials, and Pb-Se-Sn is also a subsystem of various promising thermoelectric materials.<sup>4–10</sup>

Phase diagrams provide basic material phase equilibria information. They are fundamentally important for the design and development of materials, processing route determination and product reliability assessments. Experimental results and CALPHAD-type modeling of phase diagrams of Pb-

Se, Pb-Sn and Se-Sn binary systems have been reported,<sup>11–16</sup> but there are only very limited studies of the Pb-Se-Sn phase diagrams,<sup>17–19</sup> and no phase diagrams exist for the Pb-Se-Sn ternary system of the entire compositional regime. In the present study, experimental measurements are carried out to determine the Pb-Se-Sn phase equilibria isothermal sections at 350°C and 500°C.

## EXPERIMENTAL PROCEDURES

Pb-Se-Sn alloys were prepared with pure constituent elements, Pb (99.999 wt.%, Alfa Aesar, USA), Se (99.999 wt.%, Alfa Aesar, USA) and Sn (99.99 wt.%, Alfa Aesar, USA). Stoichiometric amounts of elements were weighed using an electronic balance with 0.1 mg accuracy (Mettler, AE200, USA), and the total amount of the prepared alloy was about 1 g. They were then sealed in a quartz capsule in a 10<sup>−5</sup> bar vacuum.

Sample capsules were heated to 800°C to ensure complete melting and mixing of these constituent elements. Sample tubes were quenched in ice water and then placed back in a furnace at 350°C and 500°C for 1 to 8 months to equilibrate the alloys. The sample capsules were removed from the

furnace and quenched in water. The equilibrated alloys were removed from broken capsules and cut into two halves.

One half was ground into powder for x-ray diffraction (XRD, Scintac, XDS-2000 V/H, USA). The other half was mounted, polished and metallographically examined. Microstructures were examined using optical microscopy and scanning electron microscopy (SEM, Jeol, JSM-5600, Japan). The composition of the alloys was measured using electron probe microanalysis (EPMA, Jeol, JXA-8500F, Japan) with a WDS (wave-dispersive spectrometer). The voltage was 15.0 kV and current density was  $2 \times 10^{-8}$  A. ZAF (absorption factor *A*, atomic number factor *Z* and characteristic fluorescence correction *F*) calibration was used with Se, Sn and PbTe crystals as standards.

## EXPERIMENTAL RESULTS

### Pb-Se-Sn Isothermal Section at 350°C

Seventeen alloys were prepared and equilibrated at 350°C. Their composition is listed in Table I and shown in Fig. 1a. The liquid phase along the (Pb, Sn) side is referred to as “liquid,” and that near the Se corner is designated “liquid(Se).”

#### $\alpha$ -PbSe + Liquid Two-Phase Region

Figure 2a and b show respectively the BSE (back-scattered electrons) image and elemental mapping micrographs of alloy #1 (Pb-5.00 at.%Se-10.00 at.%Sn) equilibrated at 350°C for 4 months. Two-phase regions are observed. The composition of the gray phase in Fig. 2a is Pb-48.5 at.%Se-4.0 at.%Sn. Based on the binary Pb-Se phase diagram,<sup>11</sup> it is likely the  $\alpha$ -PbSe phase with 4.0 at.%Sn solubility. The bright region in Fig. 2a is a phase mixture. Its average composition, measured by area measurement, is Pb-0.5 at.%Se-10.3 at.%Sn. Based on its microstructure and the Pb-Sn phase diagram,<sup>13</sup> this bright phase region was (Pb, Sn)-rich liquid phase at 350°C. The liquid phase solidified and decomposed, and Pb and Sn phases were formed when the sample was removed from the furnace. Figure 2c is the powder x-ray diffractogram of alloy #1. The diffraction peaks of the Pb, Sn and PbSe phases are observed. These experimental results are consistent, and alloy #1 is therefore in the  $\alpha$ -PbSe + liquid two-phase region at 350°C. Similar results are observed for alloys #9, 10, 11 and 16, and they are all in the  $\alpha$ -PbSe + liquid two-phase region at 350°C.

#### $\alpha$ -PbSe + $\gamma$ -SeSn + Liquid Tie-Triangle

Figure 3a and b are the BSE image and elemental micrographs of alloy #2 (Pb-20.00 at.%Se-60.00 at.%Sn) equilibrated at 350°C for 4 months. Three-phase regions are observed. The composition of the dark phase is Pb-48.1 at.%Se-38.8 at.%Sn, and that of the bright phase is Pb-47.2 at.%Se-

16.5at.%Sn. The gray region is a phase mixture. Dal Corso et al.<sup>17</sup> examined the ( $\alpha$ -PbSe)-( $\gamma$ -SeSn) isoplethal section. They found that both  $\alpha$ -PbSe and  $\gamma$ -SeSn have very significant ternary solubilities. Based on these findings, it is likely that the bright phase is the  $\alpha$ -PbSe phase with 16.5 at.%Sn solubility, and the dark phase is the  $\gamma$ -SeSn phase with 13.1 at.%Pb solubility. The average composition of the gray phase mixture is Pb-0.3 at.%Se-79.3 at.%Sn. With similar reasoning as mentioned above, the gray phase mixture was a (Pb, Sn)-rich liquid phase at 350°C. It solidified and decomposed during quenching, and Pb and Sn phases were formed when the sample was removed from the furnace.

Figure 3c is the x-ray diffractogram of alloy #2. Since the ternary solubilities in the  $\alpha$ -PbSe and  $\gamma$ -SeSn phases are very high, their lattice constants and diffraction peaks are different from the pure binary  $\alpha$ -PbSe and  $\gamma$ -SeSn phases. By assuming ideal mixing, the lattice constants of the  $\alpha$ -PbSe with 16.5 at.%Sn solubility and  $\gamma$ -SeSn with 13.1 at.%Pb solubility are calculated to be 0.607 nm and 1.1 nm, respectively. The two strongest diffraction peaks of pure binary  $\alpha$ -PbSe and  $\gamma$ -SeSn phases are 29.13°, 41.6° and 30.46°, 31.08° in the JCPDS.<sup>20,21</sup> The calculated diffraction peaks of the two strongest peaks of the  $\alpha$ -PbSe and  $\gamma$ -SeSn phases in this study are 29.94°, 42.73° and 30.57°, 31.7°, respectively, and are shown in Table II. The calculated results are consistent with those observed in Fig. 3c. It is concluded that alloy #2 is in the  $\alpha$ -PbSe +  $\gamma$ -SeSn + liquid tie-triangle at 350°C. Similar results are observed for alloy #12, and it is also in the  $\alpha$ -PbSe +  $\gamma$ -SeSn + liquid three-phase region.

#### $\gamma$ -SeSn + Liquid Two-Phase Region

Figure 4a is a BSE micrograph of alloy #3 (Pb-25.00 at.%Se-70.00 at.%Sn) equilibrated at 350°C for 4 months. Two-phase regions are observed. The composition of the gray phase is Pb-49.0 at.%Se-47.6 at.%Sn. It is assumed that it is the  $\gamma$ -SeSn phase<sup>15</sup> with 3.4 at.%Pb solubility. The bright phase region is a phase mixture. The average composition is Pb-95.4 at.% Sn with negligible Se solubility. It is assumed that the bright region was a (Pb, Sn)-rich liquid phase at 350°C, and Pb and Sn phases formed when the sample was removed from the furnace. Figure 4b is the x-ray diffractogram of alloy #3. Diffraction peaks of  $\gamma$ -SeSn, Sn are observed, but the peak of Pb is too weak to identify. Similar results are observed for alloy #13. Figure 4c is the x-ray diffractogram of alloy #13, and the diffraction peaks of  $\gamma$ -SeSn, Sn, and Pb are observed in Fig. 4c. The results are in agreement, and alloys #3 and #13 are in the  $\gamma$ -SeSn + liquid two-phase region at 350°C.

#### Se<sub>2</sub>Sn + $\gamma$ -SeSn + Liquid(Se) Tie-Triangle

Figure 5a is a BSE micrograph of alloy #4 (Pb-60.00 at.%Se-30.00 at.%Sn). Three-phase regions

**Table I. Nominal composition and equilibrium phases of Pb-Se-Sn ternary alloys equilibrated at 350°C**

Alloy no.	Alloy composition			Composition equilibrium (at.%)			
	Pb	Se	Sn	Phase	Pb	Se	Sn
1	85	5	10	Liquid	89.2	0.5	10.3
				$\alpha$ -PbSe	47.5	48.5	4
2	20	20	60	$\alpha$ -PbSe	36.3	47.2	16.5
				$\gamma$ -SeSn	13.1	48.1	38.8
				Liquid	20.4	0.3	79.3
3	5	25	70	$\gamma$ -SeSn	3.4	49	47.6
				Liquid	4.6	0	95.4
4	10	60	30	Se <sub>2</sub> Sn	0	65.7	34.3
				$\gamma$ -SeSn	12.4	48.7	38.9
				Liquid(Se)	11.5	59.4	29.1
5	10	80	10	Liquid(Se)	10.1	79.5	10.4
6	10	70	20	Se <sub>2</sub> Sn	0	66.1	33.9
				Liquid(Se)	12	73.7	14.3
7	20	70	10	Liquid(Se)	14	75.4	10.6
				$\alpha$ -PbSe	47.3	47.2	5.5
8	20	52	28	$\alpha$ -PbSe	33.2	49.4	17.4
				$\gamma$ -SeSn	11.1	49.6	39.3
				Liquid(Se)	10.5	60.1	29.4
9	60	25	15	Liquid	75.4	0.4	24.2
				$\alpha$ -PbSe	45.4	47.1	7.5
10	70	5	25	Liquid	28.9	0.1	71
				$\alpha$ -PbSe	46.3	47.5	6.2
11	50	40	10	Liquid	70.6	0.8	28.6
				$\alpha$ -PbSe	47.9	47.5	4.6
12	15	35	50	$\gamma$ -SeSn	12.3	48.3	39.4
				$\alpha$ -PbSe	35.8	47.6	16.6
				Liquid	20.3	0.6	79.1
13	15	15	70	$\gamma$ -SeSn	11.1	47.8	41.1
				Liquid	15.8	0.2	84
14	11.5	54	34.5	Liquid(Se)	10	61.3	28.7
				$\gamma$ -SeSn	12.1	49.6	38.3
				Se <sub>2</sub> Sn	0	66.3	33.7
15	5	65	30	Liquid(Se)	12.1	61.1	26.8
				Se <sub>2</sub> Sn	0	65.6	34.4
16	50	30	20	Liquid	59	0.8	40.2
				$\alpha$ -PbSe	43.6	46.7	9.7

are observed, bright rods, dark rods and a continuous matrix with a fine microstructure. The composition of the bright rods is Pb-48.7 at.%Se-38.9 at.%Sn. It is likely that this is the  $\gamma$ -SeSn phase with 12.4 at.% Pb solubility. The composition of the dark rods is Pb-65.7 at.%Se-34.3 at.%Sn, and this is the Se<sub>2</sub>Sn phase with almost negligible Pb solubility. The experimental results of this study indicate that both the binary compounds,  $\alpha$ -PbSe and  $\gamma$ -SeSn, have significant ternary solubilities; however, the Pb solubility in the Se<sub>2</sub>Sn phase is very limited. Similar results were reported previously.<sup>17</sup>

The average composition of the region of the fine microstructure, the largest region, is Pb-59.4 at.%Se-29.1 at.%Sn. Based on the microstructure, this region was a liquid phase, and it solidified when the sample was removed from the furnace. Alloy #4 was in the Se<sub>2</sub>Sn +  $\gamma$ -SeSn + liquid(Se) tie-triangle at 350°C. Figure 5b is the powder x-ray diffractogram of alloy #4. Diffraction peaks of four phases,

Se<sub>2</sub>Sn,  $\gamma$ -SeSn, Se and  $\alpha$ -PbSe, are observed. The results indicate that there is no ternary compound, and  $\alpha$ -PbSe, Se<sub>2</sub>Sn,  $\gamma$ -SeSn and Se phases were formed during solidification. Similar results are observed for alloy #14 (Pb-54.00 at.%Se-34.50 at.%Sn). It is also in the Se<sub>2</sub>Sn +  $\gamma$ -SeSn + liquid(Se) tie-triangle.

### Liquid(Se) Single-Phase Region

Figure 6a is a BSE micrograph of alloy #5 (Pb-80.00 at.% Se-10.00 at.% Sn) equilibrated at 350°C for 3 months. Unlike all the micrographs shown above, this micrograph has a homogenous fine microstructure without a larger phase. There are three phases in this fine microstructure sample. The composition of the bright phase is Pb-48.6 at.%Se-1.0 at.%Sn, and it is the  $\alpha$ -PbSe with 1.0 at.%Sn solubility. The composition of the gray phase is Se-32.5 at.%Sn, and this gray phase is the Se<sub>2</sub>Sn phase

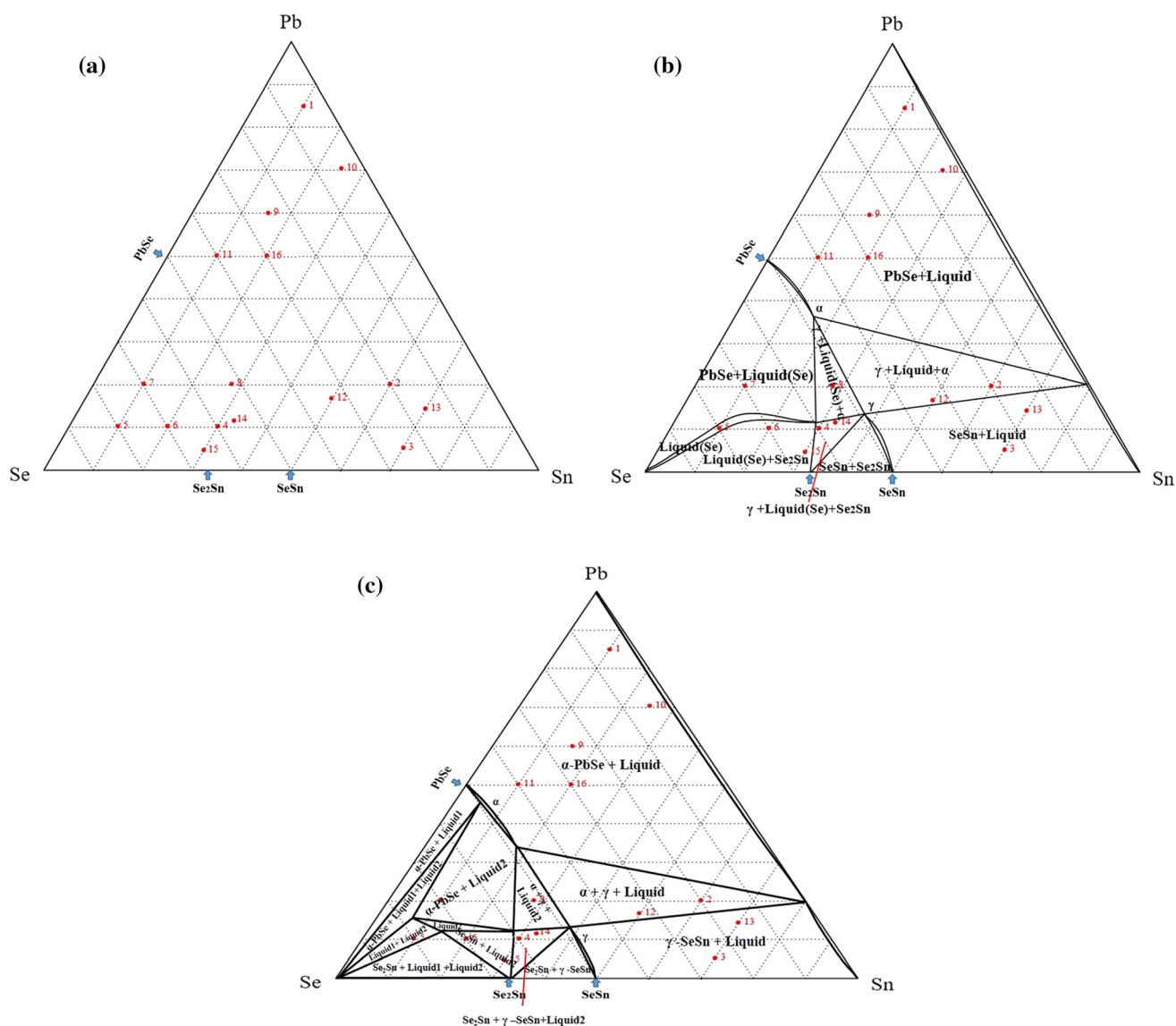


Fig. 1. Isothermal section of Pb-Se-Sn phase equilibria at 350°C: (a) superimposed with alloys examined; (b) a possible isothermal section determined in this study; (c) another possible isothermal section determined in this study.

with no noticeable Pb solubility. The composition of the dark phase is Pb-99.8 at.% Se, and the dark phase is Se with 0.2 at.% Pb solubility. Figure 6b is the powder x-ray diffractogram of alloy #5. Diffraction peaks of  $\alpha$ -PbSe, Se and  $\text{Se}_2\text{Sn}$  are observed. It is assumed that this alloy is in the liquid single-phase region, and  $\alpha$ -PbSe, Se and  $\text{Se}_2\text{Sn}$  phases were formed during solidification after the sample was removed from the furnace.

### $\text{Se}_2\text{Sn} + \text{Liquid}(\text{Se})$ Two-Phase Region

Figure 7a is the BSE micrograph of alloy #6 (Pb-70.00 at.% Se-20.00 at.% Sn) equilibrated at 350°C for 4 months. Two-phase regions are observed. The composition of the dark phase is Pb-66.1 at.% Se-33.9 at.% Sn. It is the  $\text{Se}_2\text{Sn}$ <sup>15</sup> with almost negligible Pb solubility. The continuous matrix phase region is

a phase mixture. Its average composition is Pb-73.7 at.% Se-14.3 at.% Sn. Based on the microstructure, this region was the liquid phase and it solidified during sample removal from the furnace. Figure 7b is its powder x-ray diffractogram. The diffraction peaks of three phases,  $\text{Se}_2\text{Sn}$ ,  $\alpha$ -PbSe and Se, are found. As suggested by the results of alloy #5, the liquid phase at the Se corner can form  $\text{Se}_2\text{Sn}$ ,  $\alpha$ -PbSe and Se phases during solidification. The results indicate that alloy #6 was in the  $\text{Se}_2\text{Sn} + \text{liquid}(\text{Se})$  two-phase region at 350°C, and  $\alpha$ -PbSe and Se were formed during solidification. Compared with the diffractograms of alloys #5 and 6, the intensities of the diffraction peaks of the  $\text{Se}_2\text{Sn}$  phase of alloy #6 are stronger. This is to be expected, because there is more of the  $\text{Se}_2\text{Sn}$  phase in alloy #6 than in alloy #5. Similar results are observed for



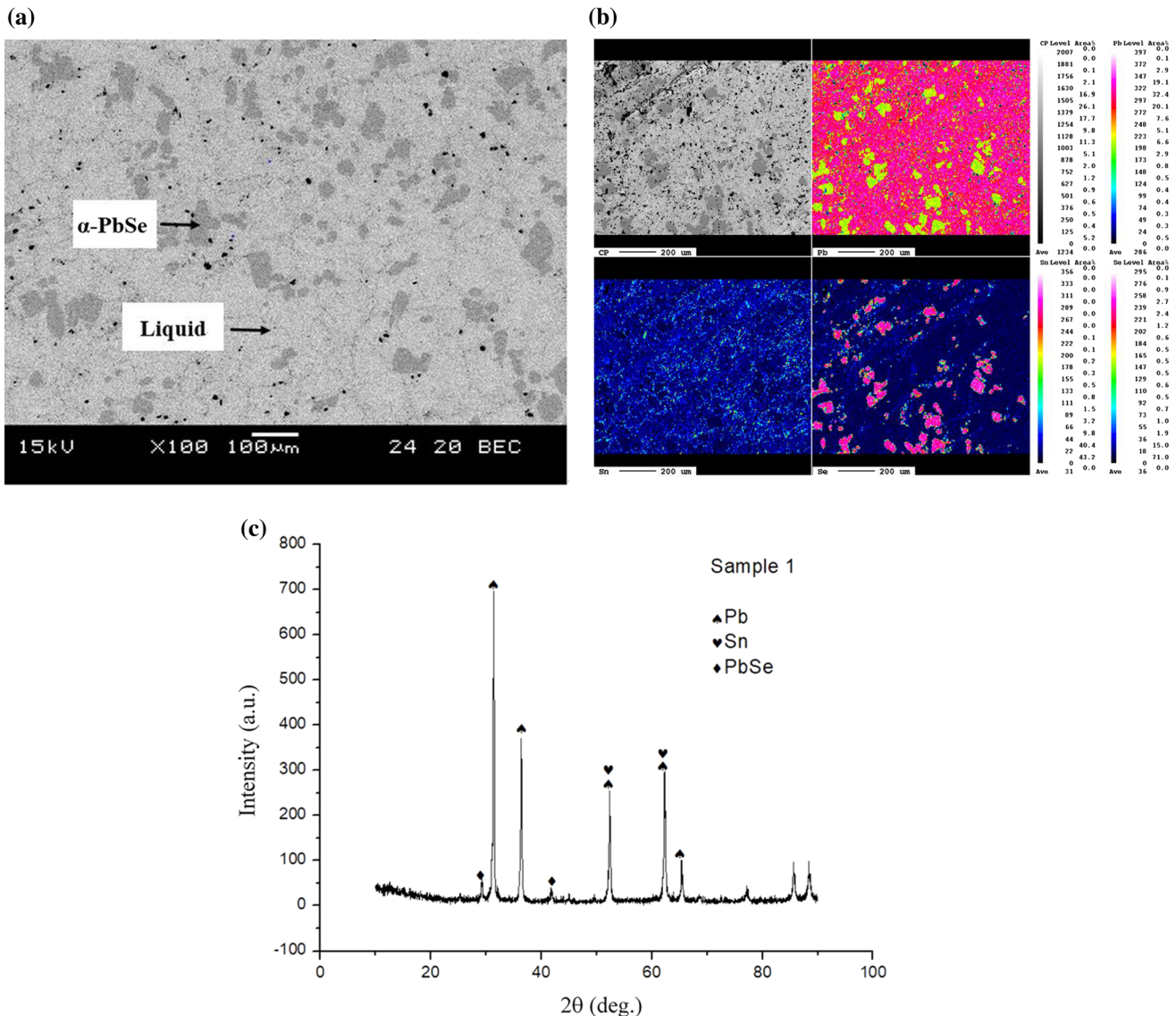


Fig. 2. Alloy #1 (Pb-5.00 at.% Se-10.00 at.% Sn) equilibrated at 350°C for 4 months: (a) BSE micrograph; (b) elemental mapping micrograph; (c) powder x-ray diffractogram.

alloy #15, and it is also in the  $\text{Se}_2\text{Sn}$  + liquid(Se) two-phase region at 350°C.

### $\alpha$ -PbSe + Liquid(Se) Two-Phase Region

Figure 8a is the BSE micrograph of alloy #7 (Pb-70.00 at.% Se-10.00 at.% Sn) equilibrated at 350°C for 4 months. The composition of the bright bulk phase is Pb-47.2 at.% Se-5.5 at.% Sn, and it is the  $\alpha$ -PbSe phase with 5.5 at.% Sn solubility. In addition to the bright bulk phase, a mixture of bright and dark phases can be observed. The darkest regions are cracks. Compositional determination of the larger dark phase indicates it is almost pure Se. The average composition of the phase mixture is Pb-75.4 at.% Se-10.6 at.% Sn. Based on the fine microstructure, the composition, the results for alloys #5 and 6, and the phase diagram of Pb-Se and Se-Sn,<sup>11,15</sup> it is concluded that the phase

mixture was the liquid phase, and alloy #7 is in the  $\alpha$ -PbSe + liquid(Se) two-phase region at 350°C. Figure 8b is the x-ray diffractogram. The diffraction peaks of  $\alpha$ -PbSe,  $\text{Se}_2\text{Sn}$  and Se are observed. As discussed previously,  $\alpha$ -PbSe,  $\text{Se}_2\text{Sn}$  and Se phases were formed during solidification, and the diffraction peaks of  $\alpha$ -PbSe are stronger than those in Fig. 6b and 7b because there is more  $\alpha$ -PbSe phase in sample alloy #7.

### $\gamma$ -SeSn + $\alpha$ -PbSe + Liquid(Se) Tie-Triangle

Figure 9a is the BSE micrograph of alloy #8 (Pb-52.00 at.% Se-28.00 at.% Sn) equilibrated at 350°C for 7 months. Three-phase regions are observed, a bright bulk phase, a gray bulk phase and a phase mixture. The composition of the bright bulk phase is Pb-49.4 at.% Se-17.4 at.% Sn and this is the  $\alpha$ -PbSe phase with significant 17.4 at.% Sn solubility. The

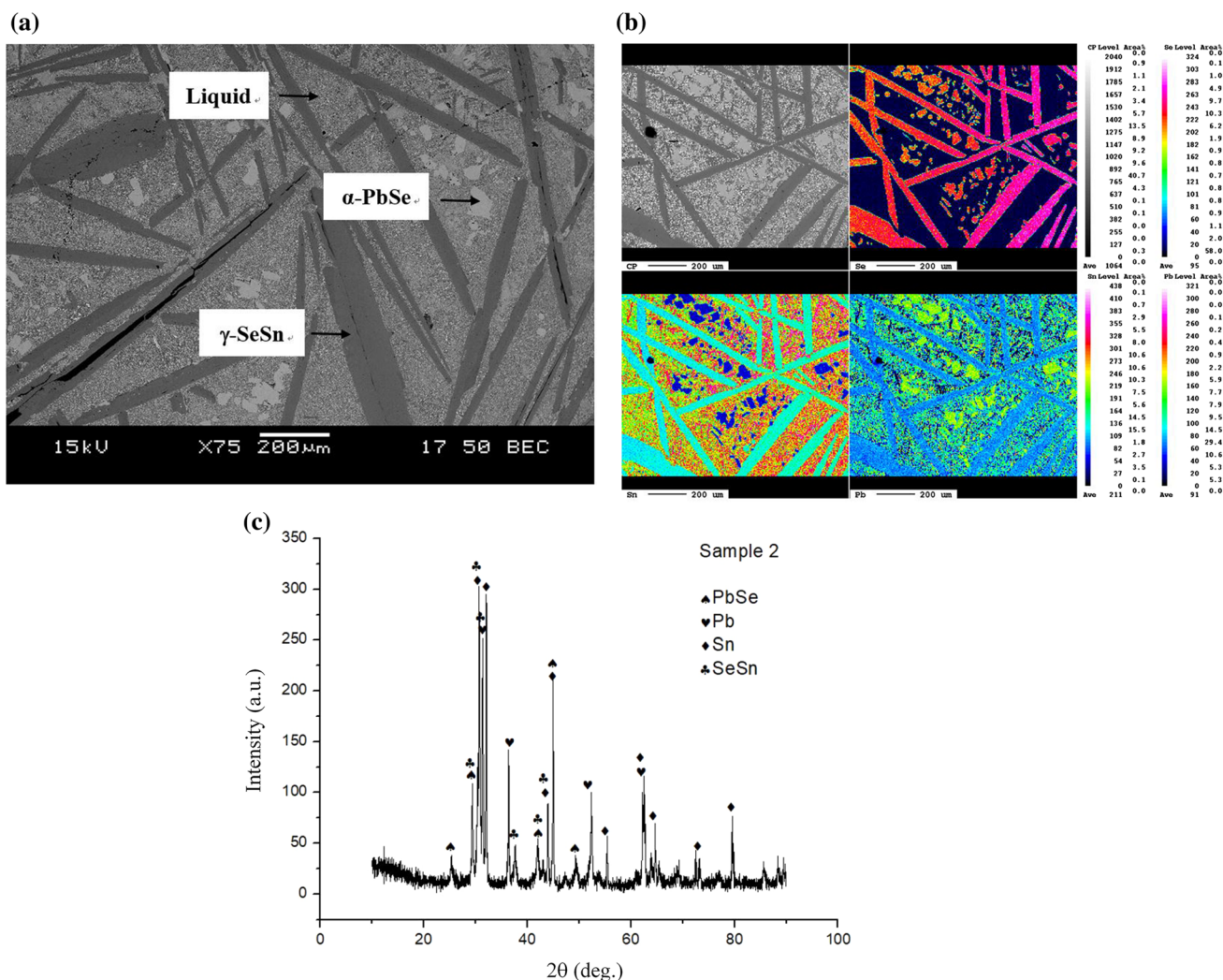


Fig. 3. Alloy #2 (Pb-20.00 at.%Se-60.00 at.%Sn) equilibrated at 350°C for 4 months: (a) BSE micrograph; (b) elemental mapping micrograph; (c) powder x-ray diffractogram.

**Table II. The calculated diffraction peaks of the two strongest peaks of each sample at 350°C**

Alloy no.	Phase	Main peak	Second peak
1	PbSe	29.17°	41.83°
2	PbSe	29.94°	42.73°
	SeSn	30.57°	31.7°
3	SeSn	30.46°	31.26°
4	SeSn	30.58°	31.8°
7	PbSe	29.29°	42.02°
8	PbSe	29.99°	42.8°
	SeSn	30.58°	31.8°
10	PbSe	29.22°	41.88°
12	PbSe	29.94°	42.73°
	SeSn	30.57°	31.7°
13	SeSn	30.56°	31.7°
14	SeSn	30.58°	31.8°

composition of the gray phase is Pb- 49.6 at.%Se-39.3 at.%Sn, and this is the  $\gamma$ -SeSn phase with 11.1 at.%Pb solubility. The average composition of the phase mixture is Pb-60.1 at.% Se-29.4 at.% Sn. Based on similar reasoning, it is concluded that the phase mixture was liquid at 350°C and that alloy #8 is in the  $\gamma$ -SeSn +  $\alpha$ -PbSe + liquid(Se) tie-triangle. Figure 9b is the x-ray diffractogram. The diffraction peaks of Se, Se<sub>2</sub>Sn,  $\alpha$ -PbSe and  $\gamma$ -SeSn are observed. Since ternary solubilities in both the  $\alpha$ -PbSe and  $\gamma$ -SeSn phases are significant, the peak shifts resulting from alloying affects are calculated by assuming an ideal mixture. The calculated first and second strongest peaks of the  $\alpha$ -PbSe and  $\gamma$ -SeSn are at 29.99°, 42.8° and 30.58°, 31.8° instead of 29.13°, 41.6° and 30.46°, 31.08° as in the case of pure  $\alpha$ -PbSe and  $\gamma$ -SeSn in the JCPDS.<sup>20,21</sup> The diffraction

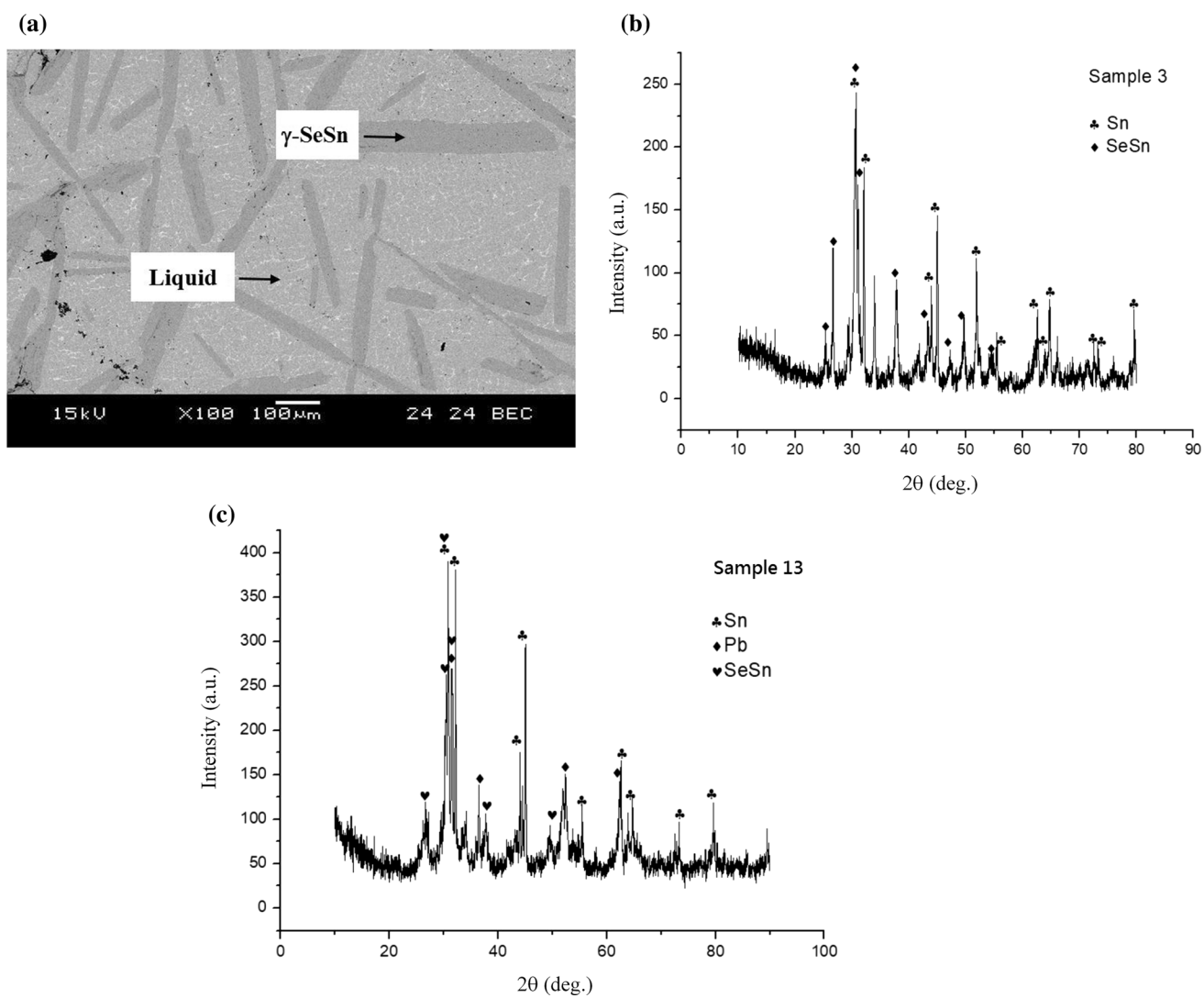


Fig. 4. Alloy #3 (Pb-25.00 at.% Se-70.00 at.% Sn) equilibrated at 350°C for 4 months: (a) BSE micrograph; (b) powder x-ray diffractogram. (c) powder x-ray diffractogram of alloy #13.

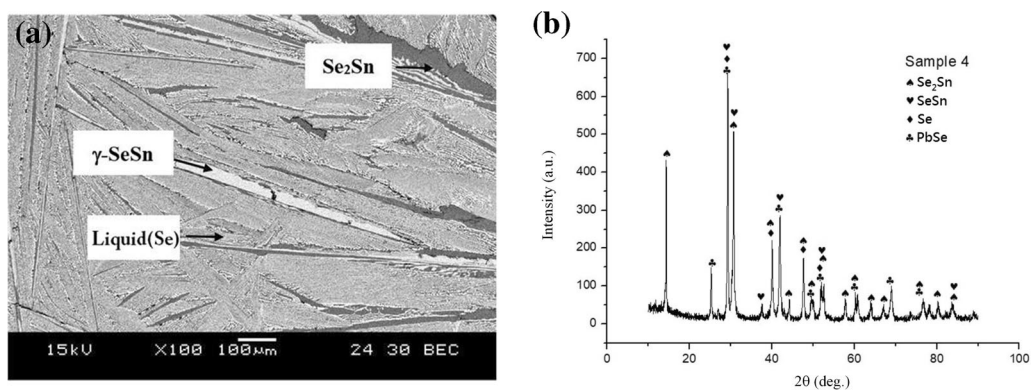


Fig. 5. Alloy #4 (Pb-60.00 at.% Se-30.00 at.% Sn) equilibrated at 350°C for 4 months: (a) BSE micrograph; (b) powder x-ray diffractogram.



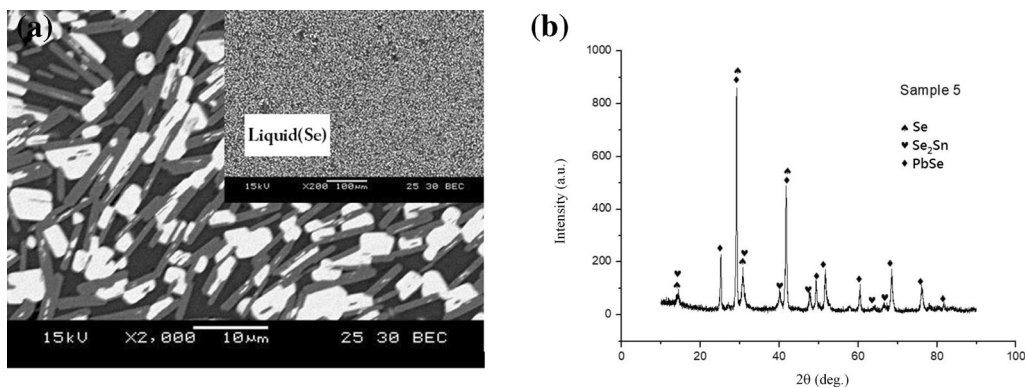


Fig. 6. Alloy #5 (Pb-80.00 at.% Se-10.00 at.% Sn) equilibrated at 350°C for 3 months: (a) BSE micrograph; (b) powder x-ray diffractogram.

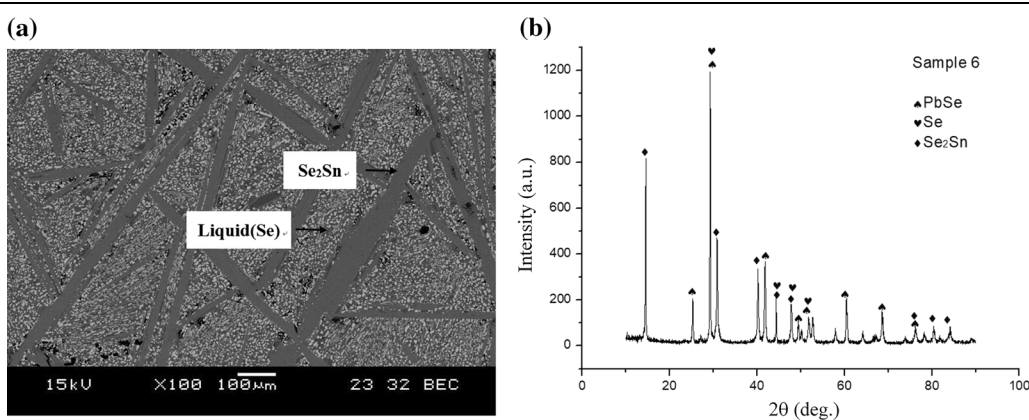


Fig. 7. Alloy #6 (Pb-70.00 at.% Se-20.00 at.% Sn) equilibrated at 350°C for 4 months: (a) BSE micrograph; (b) powder x-ray diffractogram.

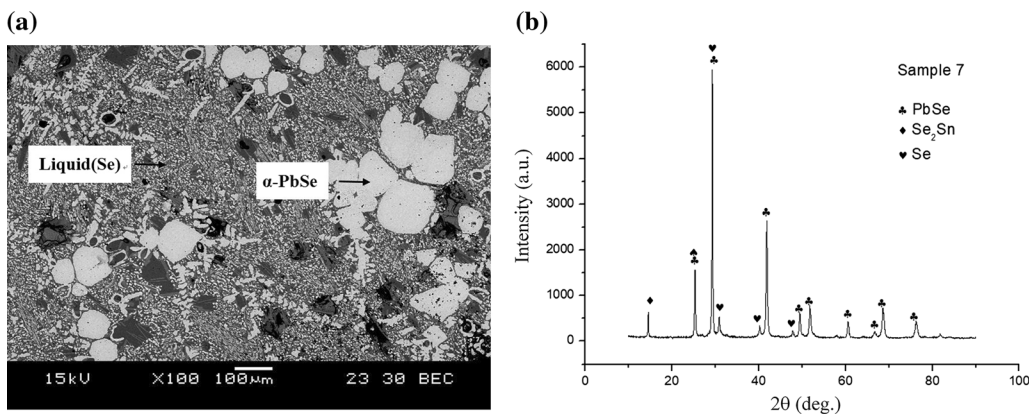


Fig. 8. Alloy #7 (Pb-70.00 at.% Se-10.00 at.% Sn) equilibrated at 350°C for 4 months: (a) BSE micrograph; (b) powder x-ray diffractogram.

peaks shown in Fig. 9b are consistent with the calculated results based on ideal mixing alloying effects.

### Pb-Se-Sn Isothermal Section at 500°C

Seventeen alloys were prepared and equilibrated at 500°C. Their composition is listed in Table III and shown in Fig. 10a.

### $\alpha$ -PbSe + Liquid Two-Phase Region

Figure 11a is the BSE micrograph of alloy #17 (Pb-22.00 at.% Se-42.00 at.% Sn) equilibrated at 500°C for 3 months. Two-phase regions are observed. The composition of the gray phase in Fig. 11a is Pb-49.2 at.%Se-15.1 at.%Sn. Based on the binary Pb-Se phase diagram,<sup>11</sup> it is likely the  $\alpha$ -PbSe phase with 15.1 at.% Sn solubility. The fine structure region in Fig. 11a is a phase mixture. The



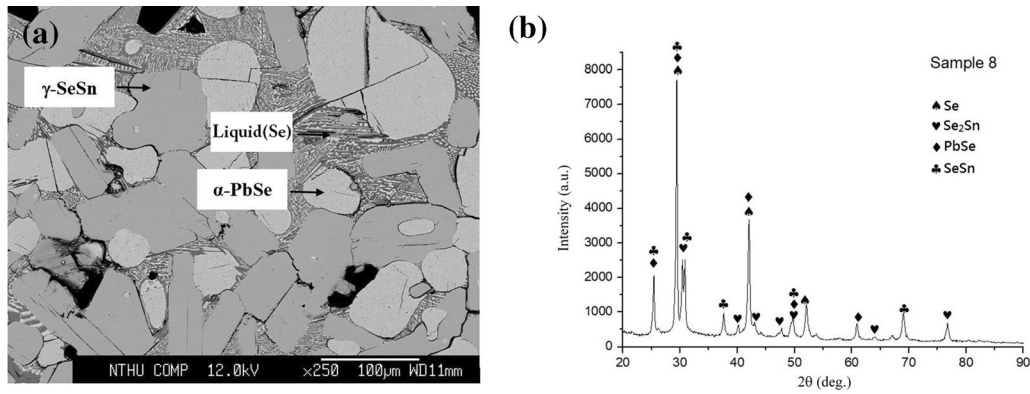


Fig. 9. Alloy #8 (Pb-52.00 at.% Se-28.00 at.% Sn) equilibrated at 350°C for 7 months: (a) BSE micrograph; (b) powder x-ray diffractogram.

Table III. Nominal composition and equilibrium phases of Pb-Se-Sn ternary alloys equilibrated at 500°C

Alloy no.	Alloy composition			Composition equilibrium (at.%)			
	Pb	Se	Sn	Phase	Pb	Se	Sn
17	36	22	42	Liquid	34.9	0	65.1
				$\alpha$ -PbSe	35.7	49.2	15.1
18	20	30	50	Liquid	22.6	0	77.4
				$\alpha$ -PbSe	31.1	47.5	21.4
				$\gamma$ -SeSn	12.8	48.6	38.6
19	10	20	70	Liquid	10.5	0.2	89.3
				$\gamma$ -SeSn	8.3	49	42.7
20	7.5	60	32.5	Liquid(Se)	10.5	59.7	29.8
				$\text{Se}_2\text{Sn}$	0	65.3	34.7
				$\gamma$ -SeSn	11.8	49	39.2
21	10	80	10	Liquid(Se)	9.7	78.7	11.6
22	5	67.5	27.5	Liquid(Se)	13.3	66.5	20.2
				$\text{Se}_2\text{Sn}$	0	66.2	33.8
23	15	80	5	Liquid(Se)	0	96.8	3.2
				$\alpha$ -PbSe	46.4	49.2	4.4
24	17.5	52.5	30	Liquid(Se)	10.7	60.2	29.1
				$\alpha$ -PbSe	27.1	49.4	23.5
				$\gamma$ -SeSn	12.1	50.3	37.6
25	70	10	20	Liquid	69.5	0	30.5
				$\alpha$ -PbSe	43.4	48.7	7.9
26	50	20	30	Liquid	49.1	0.1	50.8
				$\alpha$ -PbSe	36.6	50.3	13.1
27	30	20	50	Liquid	27.5	0.1	72.4
				$\alpha$ -PbSe	32.1	49.2	18.7
28	20	25	55	Liquid	24.1	0.2	75.7
				$\alpha$ -PbSe	30	47.9	22.1
				$\gamma$ -SeSn	14.5	47.5	38
29	10	60	30	Liquid(Se)	10.2	60.4	29.4
				$\gamma$ -SeSn	12.9	49.6	37.5
30	5	70	25	Liquid(Se)	9	79	12
				$\text{Se}_2\text{Sn}$	0	66	34
31	5	80	15	Liquid(Se)	4.1	83.1	12.8
				$\text{Se}_2\text{Sn}$	0	66.1	33.9
32	25	60	15	Liquid(Se)	16.2	64.4	19.4
				$\alpha$ -PbSe	47.5	46.9	5.6
				$\alpha$ -PbSe	27.3	49.4	23.3
33	20	51	29	$\gamma$ -SeSn	12.8	49.8	37.4

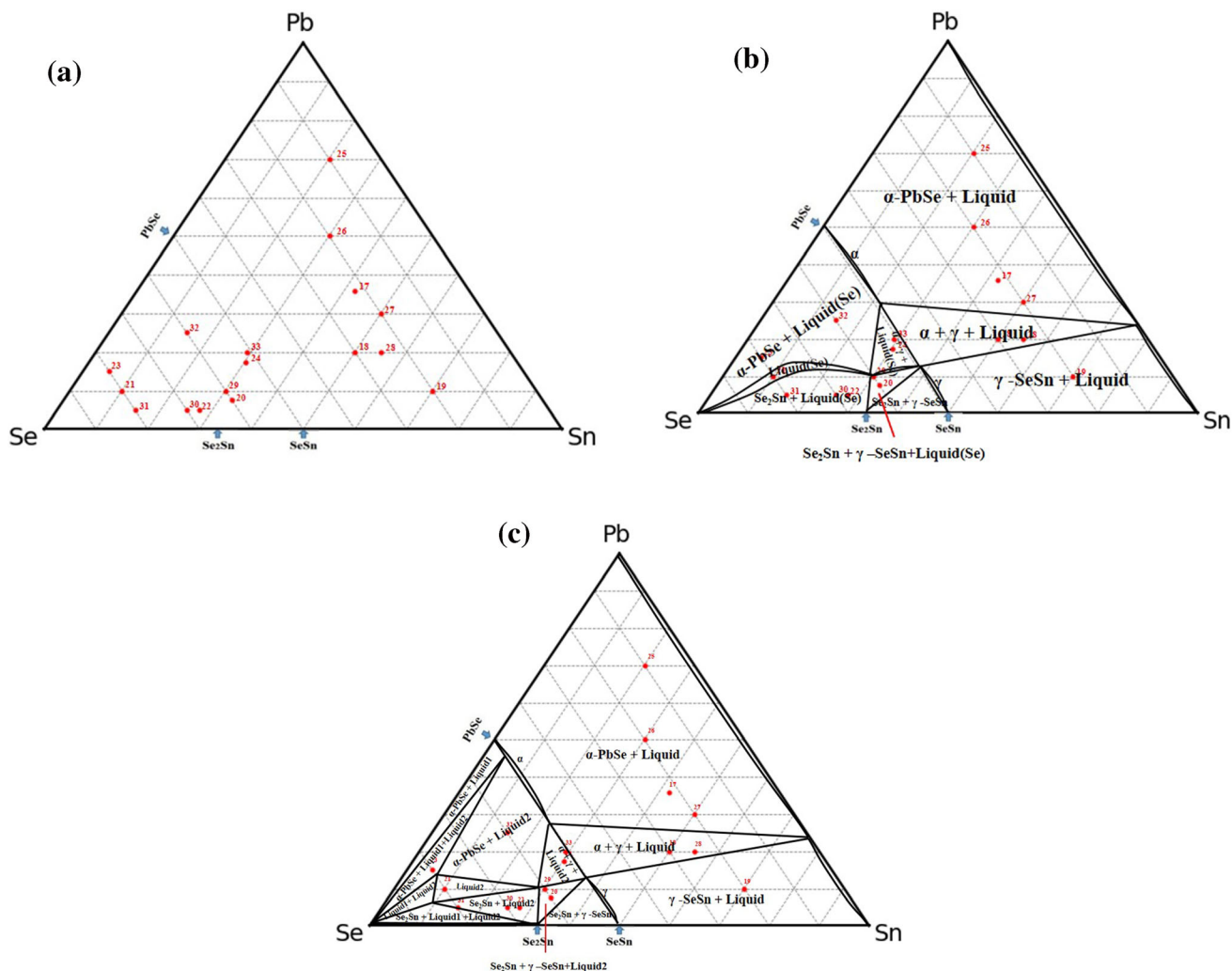


Fig. 10. Isothermal section of Pb-Se-Sn phase equilibria at 500°C: (a) superimposed with alloys examined; (b) a possible isothermal section determined in this study; (c) another possible isothermal section determined in this study.

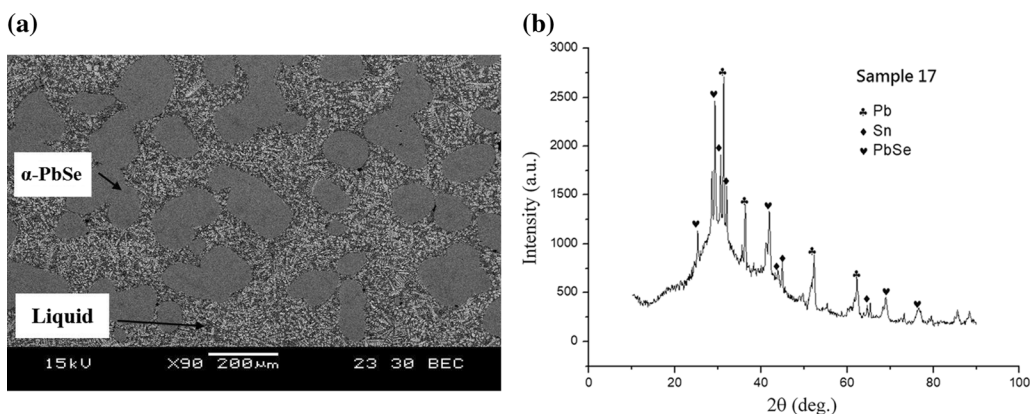


Fig. 11. Alloy #17 (Pb-22.00 at.% Se-42.00 at.% Sn) equilibrated at 500°C for 3 months: (a) BSE micrograph; (b) powder x-ray diffractogram.

average composition is Pb-65.1 at.%Sn. Based on the microstructure and the Pb-Sn phase diagram,<sup>13</sup> this fine structure phase region was a liquid phase at 500°C. The liquid phase solidified, and Pb and Sn

phases were formed when the sample was removed from the furnace. Figure 11b is the powder x-ray diffractogram of alloy #17. The diffraction peaks of Pb, Sn and  $\alpha$ -PbSe phases are observed. These

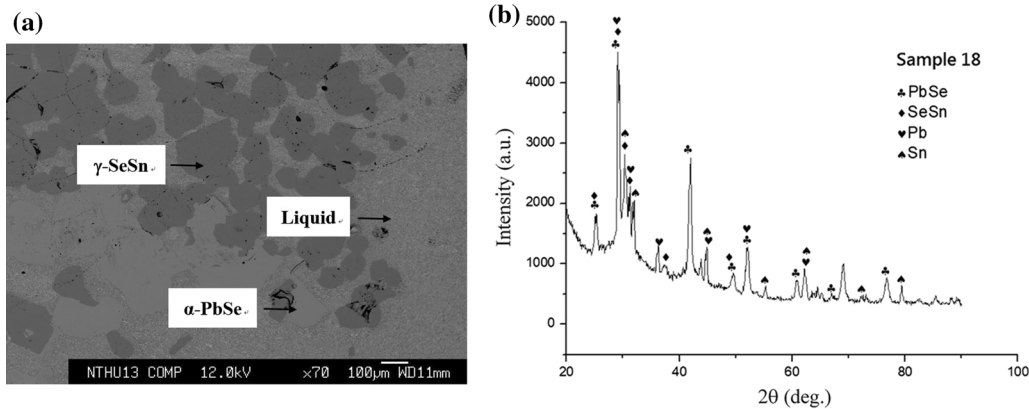


Fig. 12. Alloy #18 (Pb-30.00 at.%Se-50.00 at.%Sn) equilibrated at 500°C for 3 months: (a) BSE micrograph; (b) powder x-ray diffractogram.

**Table IV. The calculated diffractions peaks of the two strongest peaks of each sample at 500°C**

Alloy no.	Phase	Main peak	Second peak
17	PbSe	29.88°	42.67°
18	PbSe	30.18°	43°
	SeSn	30.58°	31.82°
19	SeSn	30.52°	31.55°
20	SeSn	30.57°	31.76°
23	PbSe	29.24°	41.97°
24	PbSe	29.7°	42.47°
	SeSn	30.75°	32.6°
25	PbSe	29.44°	42.18°
26	PbSe	29.77°	42.54°
27	PbSe	30.07°	42.89°
29	SeSn	30.59°	31.8°
32	PbSe	29.3°	42.03°
33	PbSe	30.34°	43.17°
	SeSn	30.59°	31.84°

experimental results are consistent, and alloy #17 is in the  $\alpha$ -PbSe + liquid two-phase region at 500°C. Similar results are observed for alloys #25–27, and they are all in the  $\alpha$ -PbSe + liquid two-phase region at 500°C.

#### $\alpha$ -PbSe + $\gamma$ -SeSn + Liquid Tie-Triangle

Figure 12a is the BSE micrograph of alloy #18 (Pb-30.00 at.%Se-50.00 at.%Sn) equilibrated at 500°C for 3 months. Three-phase regions are observed. The composition of the bright phase is Pb-47.5 at.%Se-21.4 at.%Sn, and it is the  $\alpha$ -PbSe phase with significant 21.4 at.%Sn solubility. The composition of the dark phase is Pb-48.6 at.%Se-38.6 at.%Sn, and it is the  $\gamma$ -SeSn phase with 12.8 at.% Pb solubility. The average composition of the gray phase mixture is Pb-77.4 at.% Sn. With similar reasoning as mentioned above, the gray phase mixture was a liquid phase at 500°C. It

solidified, and Pb and Sn phases were formed when the sample was removed from the furnace.

Figure 12b is the x-ray diffractogram of alloy #18. By assuming ideal mixing, the lattice constants of the  $\alpha$ -PbSe with 21.4 at.%Sn solubility and  $\gamma$ -SeSn with 12.8 at.%Pb solubility are calculated to be 0.606 nm and 1.1 nm, respectively. The two strongest diffraction peaks of pure binary  $\alpha$ -PbSe and  $\gamma$ -SeSn phases are 29.13°, 41.6° and 30.46°, 31.08° in the JCPDS.<sup>20,21</sup> The calculated diffractions peaks of the two strongest peaks of the  $\alpha$ -PbSe and  $\gamma$ -SeSn phases in this study are 30.18°, 43.0° and 30.58°, 31.82°, respectively, and are shown in Table IV. The results are consistent with those observed in Fig. 12b. It is concluded that alloy #18 is in the  $\alpha$ -PbSe +  $\gamma$ -SeSn + liquid tie-triangle at 500°C. Similar results are observed for alloy #28, and it is also in the  $\alpha$ -PbSe +  $\gamma$ -SeSn + liquid three-phase region.

#### $\gamma$ -SeSn + Liquid Two-Phase Region

Figure 13a is a BSE micrograph of alloy #19 (Pb-20.00 at.% Se-70.00 at.% Sn) equilibrated at 500°C for 3 months. Two-phase regions are observed. The composition of the gray phase is Pb-49.0 at.% Se-42.7 at.% Sn. It is assumed that it is the  $\gamma$ -SeSn phase<sup>15</sup> with 8.4 at.%Pb solubility. The fine structure phase region is a phase mixture. The average composition is Pb-89.3 at.%Sn with 0.2 at.% Se solubility. It is assumed that the fine structure region was a liquid phase at 500°C before the sample was removed from the furnace. Figure 13b is the x-ray diffractogram of alloy #19. Diffraction peaks of  $\gamma$ -SeSn, Sn and Pb are observed. The results are in agreement, and alloy #19 is in the  $\gamma$ -SeSn + liquid two-phase region at 500°C.

#### Se<sub>2</sub>Sn + $\gamma$ -SeSn + Liquid(Se) Tie-Triangle

Figure 14a is a BSE micrograph of alloy #20 (Pb-60.00 at.%Se-32.50 at.%Sn). Three-phase regions are observed, a bright bulk phase, a dark needle-like phase, and a continuous matrix with fine microstructure. The composition of the bright bulk

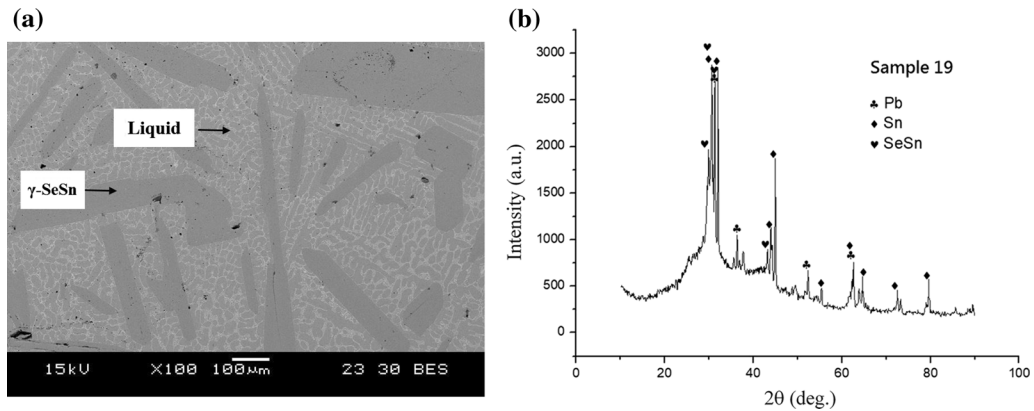


Fig. 13. Alloy #19 (Pb-20.00 at.% Se-70.00 at.% Sn) equilibrated at 500°C for 3 months: (a) BSE micrograph; (b) powder x-ray diffractogram.

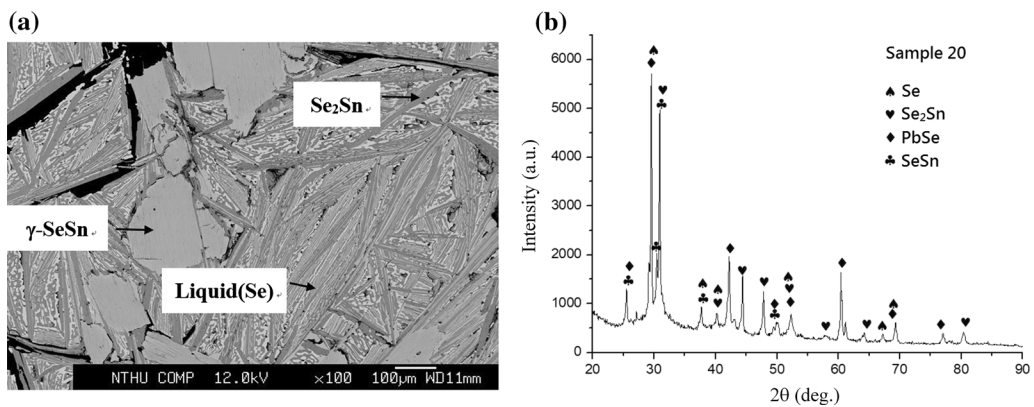


Fig. 14. Alloy #20 (Pb-60.00 at.% Se-32.50 at.% Sn) equilibrated at 500°C for 3 months: (a) BSE micrograph; (b) powder x-ray diffractogram.

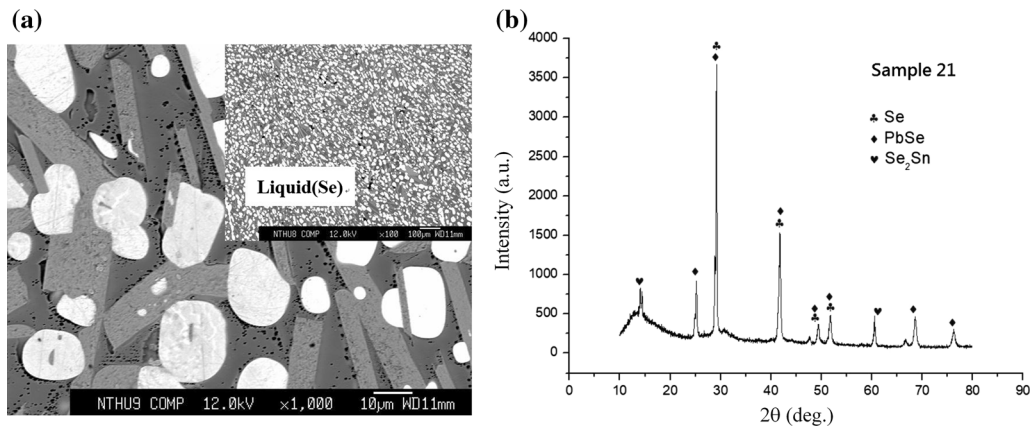


Fig. 15. Alloy #21 (Pb-80.00 at.% Se-10.00 at.% Sn) equilibrated at 500°C for 1 month: (a) BSE micrograph; (b) powder x-ray diffractogram.

phase is Pb-49.0 at.% Se-39.2 at.% Sn. This is likely the  $\gamma$ -SeSn phase with 11.8 at.% Pb solubility. The composition of the dark needle-like phase is Pb-65.3 at.% Se-34.7 at.% Sn, and this is the  $\text{Se}_2\text{Sn}$  phase with negligible Pb solubility. The average composition of the region of the fine microstructure is Pb-59.7 at.% Se-29.8 at.% Sn. Based on the microstructure, this region was the liquid phase, and it

solidified when the sample was removed from the furnace. Alloy #20 was in the  $\text{Se}_2\text{Sn} + \gamma\text{-SeSn} + \text{liquid(Se)}$  tie-triangle at 500°C. Figure 14b is the powder x-ray diffractogram of alloy #20. Diffraction peaks of four phases,  $\text{Se}_2\text{Sn}$ ,  $\gamma\text{-SeSn}$ , Se and  $\alpha\text{-PbSe}$ , are observed. The results indicate that there is no ternary compound, and  $\alpha\text{-PbSe}$ ,  $\text{Se}_2\text{Sn}$ ,  $\gamma\text{-SeSn}$  and Se phases were formed during solidification.



### Liquid(Se) Single-Phase Region

Figure 15a is a BSE micrograph of alloy #21 (Pb-80.00 at.% Se-10.00 at.% Sn) equilibrated at 500°C for 1 month. Similar to alloy #5 at 350°C, this micrograph has a homogenous fine microstructure without a larger phase. There are three phases across this region. The composition of the bright phase is Pb-50.3 at.% Se-5.1 at.% Sn, and this is the  $\alpha$ -PbSe with 5.1 at.% Sn solubility. The composition of the gray phase is Se-32.2 at.% Sn, and the gray phase is the  $\text{Se}_2\text{Sn}$  phase with no noticeable Pb solubility. The composition of the dark phase is Pb-99.3 at.% Se, and the dark phase is Se with 0.7 at.% Pb solubility. Figure 15b is the powder x-ray diffractogram of alloy #21. Diffraction peaks of  $\alpha$ -PbSe, Se and  $\text{Se}_2\text{Sn}$  are observed. It is concluded that this alloy was in the liquid single-phase region, and  $\alpha$ -PbSe, Se and  $\text{Se}_2\text{Sn}$  phases were formed when the sample was removed from the furnace.

### $\text{Se}_2\text{Sn}$ + Liquid(Se) Two-Phase Region

Figure 16a is the BSE micrograph of alloy #22 (Pb-67.50 at.% Se-27.50 at.% Sn) equilibrated at 500°C for 3 months. Two-phase regions are observed. The composition of the dark phase is Pb-66.2 at.% Se-33.8 at.% Sn. It is the  $\text{Se}_2\text{Sn}$ <sup>15</sup> with almost negligible Pb solubility. The matrix phase region is a phase mixture. Its average composition is Pb-66.5 at.% Se-20.2 at.% Sn. Based on the microstructure, this region was the liquid phase, and it solidified when it was removed from the furnace. Figure 16b is its powder x-ray diffractogram. The diffraction peaks of the three phases are  $\text{Se}_2\text{Sn}$ ,  $\alpha$ -PbSe and Se. The results indicate that alloy #22 was in the  $\text{Se}_2\text{Sn}$  + liquid(Se) two-phase region at 500°C, and the  $\alpha$ -PbSe and Se were formed during solidification. Compared with the diffractograms of alloys #21 and 22, the intensities of the diffraction peaks of the  $\text{Se}_2\text{Sn}$  phase of alloy #22 are

stronger. This is to be expected, because there is more  $\text{Se}_2\text{Sn}$  phase in alloy #22 than in alloy #21. Similar results are observed for alloys #30 and #31, and they are also in the  $\text{Se}_2\text{Sn}$  + liquid(Se) two-phase region.

### $\alpha$ -PbSe + Liquid(Se) Two-Phase Region

Figure 17a is the BSE micrograph of alloy #23 (Pb-80.00 at.% Se-5.00 at.% Sn) equilibrated at 500°C for 3 months. Two-phase regions are observed, a bright bulk phase and a phase mixture. The composition of the bright bulk phase is Pb-49.2 at.% Se-4.4 at.% Sn, and it is the  $\alpha$ -PbSe phase with 4.4 at.% Sn solubility. The average composition of the phase mixture is Pb-96.8 at.% Se-3.2 at.% Sn. Based on the fine microstructure, the results for alloys #21 and 22, and the phase diagram of Pb-Se and Se-Sn,<sup>11,15</sup> the phase mixture was the liquid phase, and alloy #23 is in the  $\alpha$ -PbSe + liquid(Se) two-phase region when at 500°C. Figure 17b is the x-ray diffractogram. Diffraction peaks of  $\alpha$ -PbSe,  $\text{Se}_2\text{Sn}$  and Se are observed. As discussed previously,  $\alpha$ -PbSe,  $\text{Se}_2\text{Sn}$  and Se phases were formed during solidification, and the intensities of the diffraction peaks of  $\alpha$ -PbSe are stronger than those in Fig. 15b and 16b because there is more  $\alpha$ -PbSe phase. Similar results are observed for alloy #32, and it is also in the  $\alpha$ -PbSe + liquid(Se) two-phase region at 500°C.

### $\gamma$ -SeSn + $\alpha$ -PbSe + Liquid(Se) Tie-Triangle

Figure 18a is the BSE micrograph of alloy #24 (Pb-52.50 at.% Se-30.00 at.% Sn) equilibrated at 500°C for 3 months. Three-phase regions are observed, a bright bulk phase, a gray bulk phase and a phase mixture. The composition of the bright bulk phase is Pb-49.4 at.% Se-23.5 at.% Sn, and it is the  $\alpha$ -PbSe phase with significant 23.5 at.% Sn solubility. The composition of the gray phase is Pb-

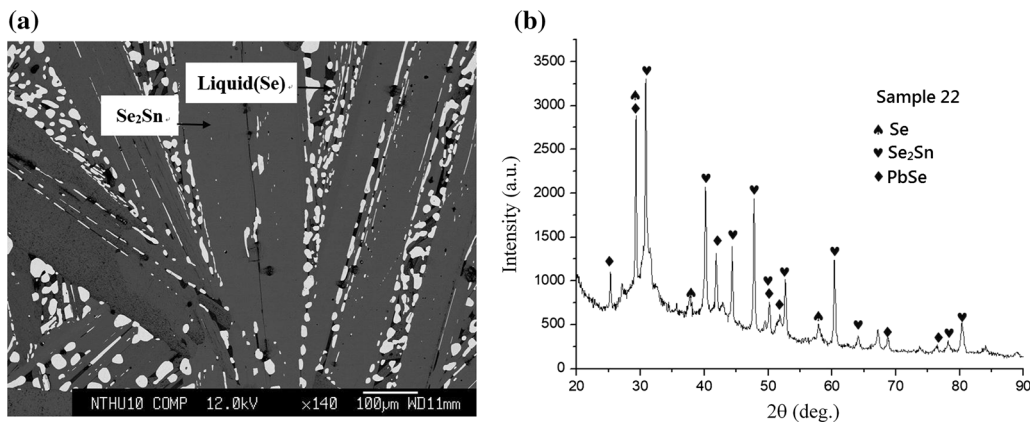


Fig. 16. Alloy #22 (Pb-67.50 at.% Se-27.50 at.% Sn) equilibrated at 500°C for 3 months: (a) BSE micrograph; (b) powder x-ray diffractogram.

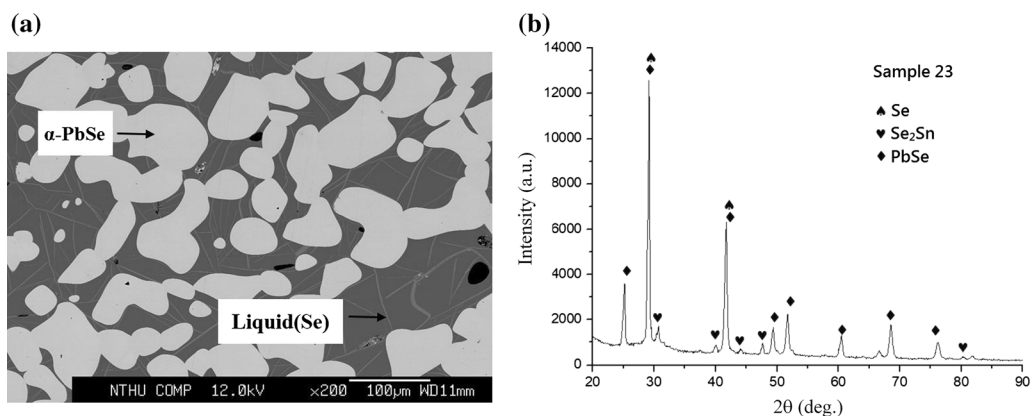


Fig. 17. Alloy #23 (Pb-80.00 at.% Se-5.00 at.% Sn) equilibrated at 500°C for 3 months: (a) BSE micrograph; (b) powder x-ray diffractogram.

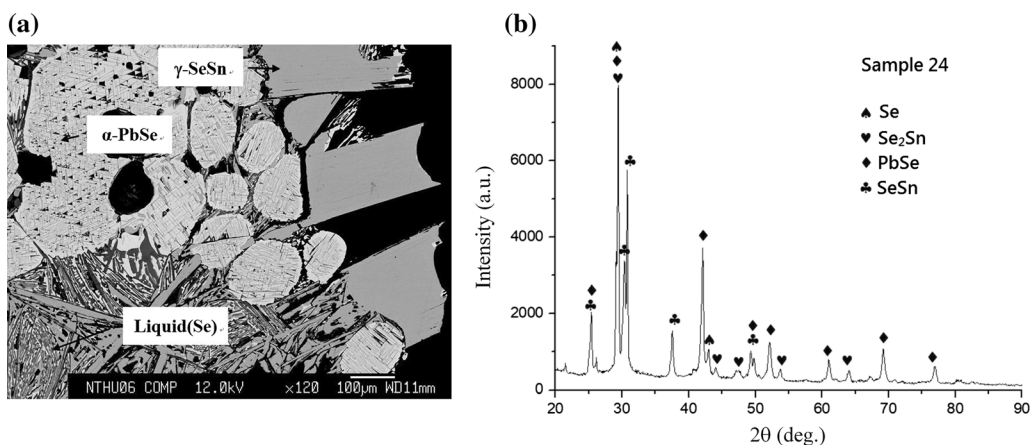


Fig. 18. Alloy #24 (Pb-52.50 at.% Se-30.00 at.% Sn) equilibrated at 500°C for 3 months: (a) BSE micrograph; (b) powder x-ray diffractogram.

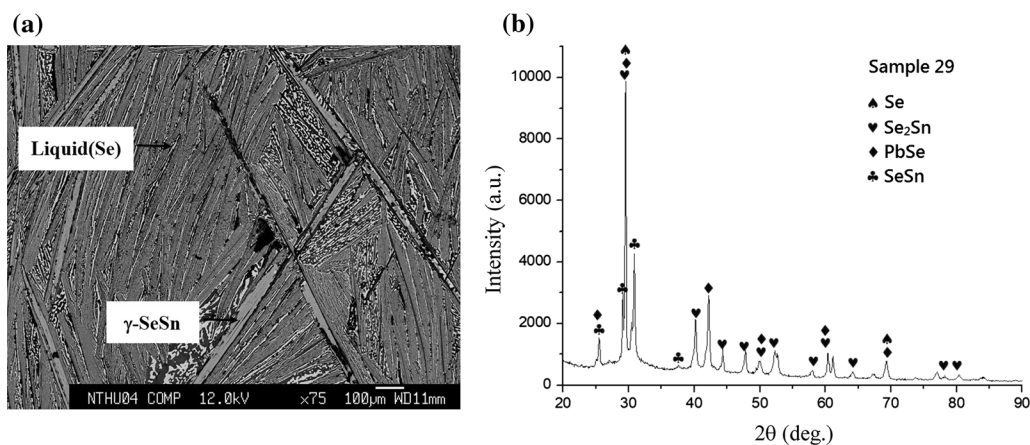


Fig. 19. Alloy #29 (Pb-60.00 at.% Se-30.00 at.% Sn) equilibrated at 500°C for 3 months: (a) BSE micrograph; (b) powder x-ray diffractogram.

50.3 at.% Se-37.6 at.% Sn, and it is the  $\gamma$ -SeSn phase with 12.1 at.% Pb solubility. The average composition of the phase mixture is Pb-60.2 at.% Se-29.1 at.% Sn. Based on similar reasoning, it is concluded that the phase mixture was liquid at 500°C, and alloy #24 is in the  $\gamma$ -SeSn +  $\alpha$ -PbSe + liquid(Se) tie-triangle. Figure 18b is the x-ray diffractogram. Diffraction peaks of Se, Se<sub>2</sub>Sn,  $\alpha$ -PbSe and  $\gamma$ -SeSn

are observed. Since ternary solubilities in both the  $\alpha$ -PbSe and  $\gamma$ -SeSn phases are significant, the peak shifts caused by the alloying affects are calculated by assuming an ideal mixture. The calculated first and second strongest peaks of the  $\alpha$ -PbSe and  $\gamma$ -SeSn are at 29.7°, 42.47° and 30.75°, 32.6° instead of 29.13°, 41.6° and 30.46°, 31.08° as in the case of the pure  $\alpha$ -PbSe and  $\gamma$ -SeSn in the JCPDS.<sup>20,21</sup> The

diffraction peaks as shown in Fig. 19b are consistent with the prediction by calculation.

### $\gamma$ -SeSn + Liquid(Se) Two-Phase Region

Figure 19a is a BSE micrograph of alloy #29 (Pb-60.00 at.%Se-30.00 at.%Sn) equilibrated at 500°C for 3 months. Two-phase regions are observed, a gray phase and a phase mixture. The composition of the gray phase is Pb-49.6 at.%Se-37.5 at.%Sn. It is assumed that it is the  $\gamma$ -SeSn phase<sup>15</sup> with 12.9 at.%Pb solubility. The average composition of the phase mixture is Pb-60.4 at.% Se-29.4 at.% Sn. Based on similar reasoning as that for alloy #23, it is concluded that the phase mixture was liquid at 500°C. Figure 19b is the x-ray diffractogram. Diffraction peaks of Se, Se<sub>2</sub>Sn,  $\alpha$ -PbSe and  $\gamma$ -SeSn are observed, and the peak shifts resulting from alloying affects are calculated by assuming an ideal mixture. The calculated first and second strongest peaks of the  $\gamma$ -SeSn are at 30.59° and 31.8° instead of 30.46°, 31.08° as in the case of pure  $\gamma$ -SeSn in the JCPDS.<sup>20,21</sup> The diffraction peaks as shown in Fig. 19b are consistent with the prediction by calculation. Alloy #29 is in the  $\gamma$ -SeSn + liquid(Se) two-phase region at 500°C.

### $\gamma$ -SeSn + $\alpha$ -PbSe Two-Phase Region

Figure 20a is a BSE micrograph of alloy #33 (Pb-51.00 at.%Se-29.00 at.%Sn) equilibrated at 500°C for 3 months. Two-phase regions are observed, a gray phase and a dark phase. It is worth mentioning that the darkest regions are not phases but holes. The composition of the gray phase is Pb-49.4 at.%Se-23.3 at.%Sn. It is assumed that it is the  $\alpha$ -PbSe phase with significant 23.3 at.%Sn solubility. The composition of the dark phase is Pb-49.8 at.%Se-37.4 at.%Sn. It is the  $\gamma$ -SeSn<sup>15</sup> with 12.8 at.%Pb solubility. Figure 20b is the x-ray

diffractogram of alloy #33. Diffraction peaks of  $\alpha$ -PbSe and  $\gamma$ -SeSn are observed, and the two strongest peaks of the  $\alpha$ -PbSe and  $\gamma$ -SeSn phases are in agreement with the calculated results, which are 30.34, 43.17 and 30.59, 31.84, shown in Table -IV. Alloy #33 is in the  $\gamma$ -SeSn +  $\alpha$ -PbSe two-phase region at 500°C.

## DISCUSSION

### Pb-Se-Sn Isothermal Section at 350°C

The Pb-Se-Sn isothermal section at 350°C can be determined by the experimental phase equilibria results of ternary alloys, as mentioned above, and the phase diagrams of the three constituent binary systems.<sup>11-16</sup> Figure 1b shows the determined isothermal section. There is no ternary compound in the Pb-Se-Sn system. There are three tie-triangles, liquid +  $\gamma$ -SeSn +  $\alpha$ -PbSe, liquid(Se) +  $\gamma$ -SeSn + Se<sub>2</sub>Sn and  $\gamma$ -SeSn +  $\alpha$ -PbSe + liquid(Se). Both  $\gamma$ -SeSn and  $\alpha$ -PbSe have very significant ternary solubility, but the Pb solubility in the Se<sub>2</sub>Sn is negligible.

As can be seen in Fig. 1b, the liquid(Se) phase region has a peculiar shape. A different illustration of the experimental results is shown in Fig. 1c. The main difference between Fig. 1b and c is that there are two liquid phases at the Se corner in Fig. 1c, but only one in Fig. 1b. The liquid phase shape is no longer strange in Fig. 1c, but there is no clear experimental evidence to support the two liquid phases. It is worth mentioning that the two liquid phases are close to the Se corner, and it is extremely difficult to examine the composition and metallography of the samples at these regions due to the high Se vapor pressure. As summarized in Table I, both isothermal sections as shown in Fig. 1b and c are possible if liquid 1 and liquid 2 cannot be clearly differentiated.

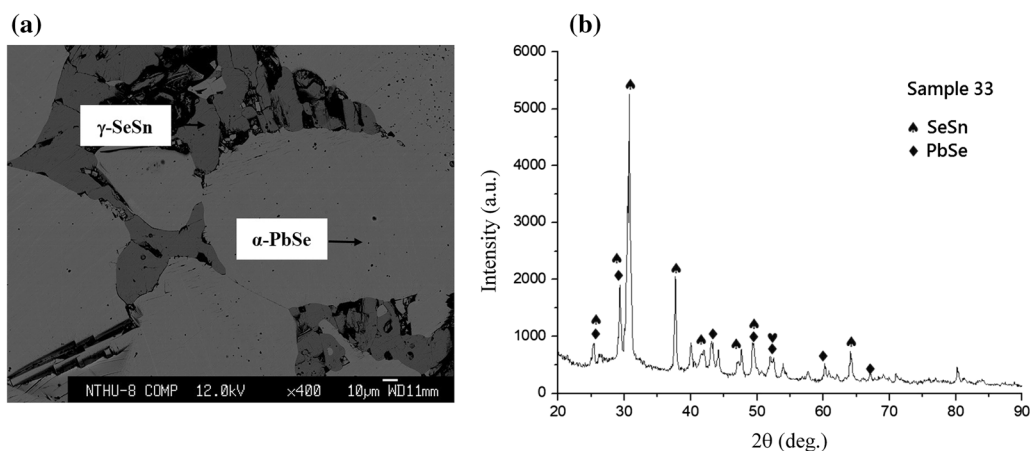


Fig. 20. Alloy #33 (Pb-51.00 at.%Se-29.00 at.%Sn) equilibrated at 500°C for 3 months: (a) BSE micrograph; (b) powder x-ray diffractogram.



### Pb-Se-Sn Isothermal Section at 500°C

The Pb-Se-Sn isothermal section at 500°C can be determined by the experimental phase equilibria results of ternary alloys, as mentioned above, and the phase diagrams of the three constituent binary systems.<sup>11–16</sup> Figure 10b and c show the two possibilities of the determined isothermal section. There is no ternary compound in the Pb-Se-Sn system. In Fig. 10b, there are three tie-triangles, liquid +  $\gamma$ -SeSn +  $\alpha$ -PbSe, liquid(Se) +  $\gamma$ -SeSn + Se<sub>2</sub>Sn and  $\gamma$ -SeSn +  $\alpha$ -PbSe + liquid(Se). The primary difference between Fig. 10b and c is if there are two liquid phases at the Se corner. Comparing the isothermal section at 350°C, the solubility of Sn in  $\alpha$ -PbSe at 500°C increases substantially, the solubility of Pb in  $\gamma$ -SeSn is about the same, and the Pb solubility in the Se<sub>2</sub>Sn remains negligible.

### The Shape and Position of the Liquid Single-Phase Region

The experimental results in the Se-rich corner indicate the existence of an extensive liquid field at both studied temperatures. The composition of the liquid phase in samples #23 and #7 in the adjacent fields  $\alpha$ -PbSe + liquid(Se) differs significantly from the position in the phase diagram. Sample #7 contains a significant amount of Sn and Pb, and the composition of the liquid phase in this sample is very close to the pure liquid sample #5. On the other hand, sample #23 is very close to the pure selenium. This, together with the phase composition of other samples in adjacent phase fields, seems to indicate a very narrow and prolonged liquid single-phase region directed towards the corner of the  $\gamma$ -SeSn +  $\alpha$ -PbSe + liquid(Se) three-phase region. This shape of the single-phase field is not very likely, and a second possibility exists: the existence of a liquid miscibility gap in the ternary phase diagram. Both Pb-Se and Se-Sn binary phase diagrams have strong tendencies to form stable and/or metastable miscibility gaps in the Se-rich region of the phase diagrams, and it is quite possible that the miscibility gap will appear in the ternary system at lower temperatures. The preliminary CALPHAD-type calculations carried out by one of the authors indicate the existence of the miscibility gap, but do not allow us to model the extremely prolonged liquid single-phase region from the pure Se-liquid to the above-mentioned three-phase region.

### CONCLUSIONS

Phase diagrams of the Pb-Se-Sn ternary system of thermoelectric importance are determined at 350°C and 500°C. No ternary compounds are observed. There are three tie-triangles: liquid +  $\gamma$ -SeSn +  $\alpha$ -PbSe, liquid(Se) +  $\gamma$ -SeSn + Se<sub>2</sub>Sn and  $\gamma$ -SeSn +  $\alpha$ -PbSe + liquid(Se).  $\gamma$ -SeSn and  $\alpha$ -PbSe have very

significant ternary solubility, but the ternary solubility in the Se<sub>2</sub>Sn is negligible. There is one unresolved issue at the Se corner. If there is only one liquid phase, the liquid-phase region has a peculiar shape. More clear evidence is needed if there are two liquid phases.

### ACKNOWLEDGMENTS

The authors acknowledge the financial support of the Ministry of Science and Technology of Taiwan (MOST 107-2923-E-007-005-MY3) and the Czech Science Foundation No. 17-12844S.

### REFERENCES

1. A. Zevalkink, D.M. Smiadak, J.L. Blackburn, A.J. Ferguson, M.L. Chabinyk, O. Delaire, J. Wang, K. Kovnir, J. Martin, L.T. Schelhas, T.D. Sparks, S.D. Kang, M.T. Dylla, G.J. Snyder, B.R. Ortiz, and E.S. Toberer, *Appl. Phys. Rev.* 5, 021303 (2018).
2. X. Zhang and L.D. Zhao, *J. Mater.* 1, 92 (2015).
3. S. LeBlanc, *Sustain. Mater. Technol.* 1, 26 (2014).
4. Z. Chen, B. Ge, W. Li, S. Lin, J. Shen, Y. Chang, R. Hanus, G.J. Snyder, and Y. Pei, *Nat. Commun.* 8, 1 (2017).
5. L.D. Zhao, G. Tan, S. Hao, J. He, Y. Pei, H. Chi, H. Wang, S. Gong, H. Xu, V.P. Dravid, C. Uher, G.J. Snyder, C. Wolverton, and M.G. Kanatzidis, *Science* 351, 141 (2016).
6. C. Chang, Q. Tan, Y. Pei, Y. Xiao, X. Zhang, Y.X. Chen, L. Zheng, S. Gong, J.F. Li, J. He, and L.D. Zhao, *RSC Adv.* 6, 98216 (2016).
7. C.F. Wu, T.R. Wei, and J.F. Li, *Phys. Chem. Chem. Phys.* 17, 13006 (2015).
8. A.A. Reijnders, J. Hamilton, V. Britto, J.B. Brubach, P. Roy, Q.D. Gibson, R.J. Cava, and K.S. Burch, *Phys. Rev. B—Condens. Matter Mater. Phys.* 90, 1 (2014).
9. T. Liang, Q. Gibson, J. Xiong, M. Hirschberger, S.P. Koduvayur, R.J. Cava, and N.P. Ong, *Nat. Commun.* 4, 1 (2013).
10. P. Dziawa, B.J. Kowalski, K. Dybko, R. Buczko, A. Szczerbakow, M. Szot, E. Łusakowska, T. Balasubramanian, B.M. Wojek, M.H. Berntsen, O. Tjernberg, and T. Story, *Nat. Mater.* 11, 1023 (2012).
11. Y. Liu, Z. Kang, G. Sheng, L. Zhang, J. Wang, and Z. Long, *J. Electron. Mater.* 41, 1915 (2012).
12. D.N. Seidnman, *Transactions Metall. Soc. AIME* 236, 1361 (1966).
13. S.K. Lin, C.K. Yeh, W. Xie, Y.C. Liu, and M. Yoshimura, *Sci. Rep.* 3, 4 (2013).
14. I. Karakaya and W.T. Thompson, *Bull. Alloy Phase Diagr.* 9, 144 (1988).
15. Y. Feutelais, M. Majid, B. Legendre, and S.G. Fries, *J. Phase Equilib.* 17, 40 (1996).
16. R.C. Sharma and Y.A. Chang, *Bull. Alloy Phase Diagr.* 7, 68 (1986).
17. S. Dal Corso, B. Liutard, and J.C. Tedenac, *J. Phase Equilib.* 16, 308 (1995).
18. Z.M. Latypov, V.P. Savel'ev, I.S. Aver'yanov, and A.S. Ul'danov, *Inorg. Mater.* 7, 1865 (1971).
19. V.T. Shtanov, V.P. Zlomanov, and A.V. Novoselova, *Inorg. Mater.* 11, 301 (1975).
20. Joint Committee on Powder Diffraction Standards (JCPDS). Card no. 06-0354 (1997).
21. Joint Committee on Powder Diffraction Standards (JCPDS). Card no. 48-1224 (1997).

**Publisher's Note** Springer Nature remains neutral with regard to jurisdictional claims in published maps and institutional affiliations.